

RESEARCH ARTICLE

Developmental deletion of amyloid precursor protein precludes transcriptional and proteomic responses to brain injury

Valentina Lacovich^{1,2} | Maria Čarna^{1,3} | Sebastian J. Novotný^{1,3} | Shanshan Wang^{4,5} |
Kateřina Texlová¹ | Kristina Locker Kovačovicova⁶ | Neda Dragišić¹ | Daniel Havas⁶ |
Brian P. Head^{4,5} | Yonas E. Geda⁷ | Clara Limbäck-Stokin⁸ | Gorazd Bernard Stokin^{1,3,9}

¹Translational Aging and Neuroscience Program, Center for Translational Medicine, International Clinical Research Center, St. Anne's University Hospital, Brno, Czech Republic

²Central European Institute of Technology at Masaryk University (CEITEC MU), Brno, Czech Republic

³Institute for Molecular and Translational Medicine, Faculty of Medicine and Dentistry, Palacký University Olomouc, Olomouc, Czech Republic

⁴Veterans Affairs San Diego Healthcare System, San Diego, California, USA

⁵Department of Anesthesiology, University of California San Diego, San Diego, California, USA

⁶PsychoGenics Inc., 215 College Road Paramus, New Jersey, New Jersey, USA

⁷Department of Neurology, Barrow Neurological Institute, Phoenix, Arizona, USA

⁸Neuropathology and Ocular Pathology Department, Oxford University Hospitals NHS Foundation Trust, Oxford, UK

⁹Department of Neurology, Royal Gloucester Hospital, Gloucestershire Hospitals NHS Foundation Trust, Gloucester, UK

Correspondence

Gorazd Bernard Stokin, Institute for Molecular and Translational Medicine, Faculty of Medicine and Dentistry, Palacký University Olomouc, Hnevotinska 1333/5, 77900 Olomouc, Czech Republic.
Email: gbstokin@alumni.ucsd.edu

Abstract

INTRODUCTION: Amyloid precursor protein (APP) undergoes striking changes following traumatic brain injury (TBI). Considering its role in the control of gene expression, we investigated whether APP regulates transcription and translation following TBI.

METHODS: We assessed brain morphology ($n = 4-9$ mice/group), transcriptome ($n = 3$ mice/group), proteome ($n = 3$ mice/group), and behavior ($n = 17-27$ mice/group) of wild-type (WT) and APP knock-out (KO) mice either untreated or 10-weeks following TBI.

RESULTS: After TBI, WT mice displayed transcriptional programs consistent with late stages of brain repair, hub genes were predicted to impact translation and brain proteome showed subtle changes. APP KO mice largely replicated this transcriptional repertoire, but showed no transcriptional nor translational response to TBI.

Valentina Lacovich, Maria Čarna, and Sebastian J. Novotný contributed equally to this study.

Funding information: European Regional Development Funds, Grant/Award Number: CZ.02.1.01/0.0/0.0/16_019/0000868; European Union's Horizon 2020, Grant/Award Number: CZ.02.1.01/0.0/0.0/17_043/0009632; CETOCOEN EXCELLENCE, Grant/Award Number: CZ.02.1.01/0.0/0.0/15_003/0000492; VA Merit, Grant/Award Number: 5101BX003671; VA Research Career Scientist Award, Grant/Award Number: 11K6BX006318; Czech Science Foundation (GAČR), Grant/Award Number: 21-27329X; European Union: Next Generation EU – Project National Institute for Neurological Research, Grant/Award Number: LX22NPO5107 (MEYS)

This is an open access article under the terms of the [Creative Commons Attribution-NonCommercial-NoDerivs](https://creativecommons.org/licenses/by-nc-nd/4.0/) License, which permits use and distribution in any medium, provided the original work is properly cited, the use is non-commercial and no modifications or adaptations are made.

© 2025 The Author(s). *Alzheimer's & Dementia* published by Wiley Periodicals LLC on behalf of Alzheimer's Association.

DISCUSSION: The similarities between WT mice following TBI and APP KO mice suggest that developmental APP deficiency induces a condition reminiscent of late stages of brain repair, hampering the control of gene expression in response to injury.

KEYWORDS

amyloid precursor protein, behavior, brain morphology, brain repair, gene expression, transcription, translation, traumatic brain injury

Highlights

- 10-weeks after TBI, brains exhibit transcriptional profiles consistent with late stage of brain repair.
- Developmental APP deficiency maintains brains perpetually in an immature state akin to late stages of brain repair.
- APP responds to TBI by changes in gene expression at a transcriptional and translational level.
- APP deficiency precludes molecular brain changes in response to TBI.

1 | BACKGROUND

The amyloid precursor protein (APP) encodes a ubiquitously expressed type I integral membrane protein.¹ Together with amyloid-like protein 1 and 2 (APLP1, APLP2) homologs,^{2,3} APP belongs to an evolutionarily conserved gene family.⁴⁻⁶ To date, all gene family members have been deleted individually or in combination in the attempt to elucidate their functions. APP knock-out (KO) mice are viable, of reduced body weight, and display behavioral deficits.^{7,8} The double and triple KO mice show different degrees of early postnatal lethality,^{9,10} indicative of functional redundancy among the APP gene family members. Circumventing the confounding effects of functional redundancy, the conditional triple APP/APLP1/APLP2 KO mice demonstrate a role of APP family members in brain development as well as in synaptic plasticity and neuronal excitability through the Kv7 potassium channels.^{11,12} This work elegantly complements previous studies suggestive of a role of APP family members at the synapse.¹³⁻¹⁷

Mechanistically, the secreted APP fragments have been proposed to exert neurotrophic activity and to exhibit neuroprotective effects,¹⁸⁻²¹ while the APP intracellular C-terminal domain (AICD) has been earmarked to control gene expression.²²⁻²⁵ A link between APP family members and transcriptional regulation has also been reported in the conditional APP/APLP1/APLP2 KO mice.²⁶ The physiological implications of this biological function of APP in controlling gene expression, however, remain largely unknown. Given that APP undergoes profound changes in its structure and distribution following traumatic brain injury (TBI),²⁷⁻³⁰ we investigated the role of APP in regulating gene expression in mice subjected to controlled cortical impact (CCI). Using behavioral, morphological, and molecular approaches, we show that APP controls transcriptional and translational events of gene expression involved in brain maturation and repair.

2 | METHODS

2.1 | Animals and tissue sample preparation

Wild-type (WT) (C57BL/6) and APP KO (B6.129S7-*App*^{tm1Dbo}/J backcrossed to C57BL/6) mice were purchased from Jackson Laboratories (Bar Harbor, ME, USA) and handled in compliance with the Guide for the Care and Use of the Laboratory Animals (National Academy of Science, Washington DC, USA). All animal use protocols were approved by the Veterans Administration San Diego Healthcare System Institutional Animal Care and Use Committee (San Diego, CA, USA). In the current study, we examined only male mice. While this approach is supportive of 3R principles,³¹ it is also a limitation of the study with its findings requiring further validation on a mixed cohort of female and male mice. Age-matched mice were housed under standard conditions with access to food and water ad libitum. Following behavioral testing, all mice were euthanized by rapid decapitation and brains were collected for the analyses. Brains were cut with half of the side ipsilateral to the CCI homogenized with 1× RIPA buffer (20–188 Millipore) for protein extraction and the other half ipsilateral to the CCI homogenized with QIAzol lysis reagent (Qiagen) for RNA extraction. Therefore, brain samples used for RNA-Seq and tandem mass tag mass spectrometry (TMT-MS) contained comparable amounts of brain tissue equally subject to CCI.

2.2 | Controlled cortical impact

The CCI mouse model replicates the mechanical forces observed in severe TBI. As previously described,³² following isoflurane anesthesia the mice were fixed into a stereotactic frame. A burr hole was made approximately 5 mm anterior to posterior (0 to –5 A-P) from the

bregmatic suture and 4 mm laterally from the sagittal suture over the right hemisphere. A craniotomy was performed with a portable drill over the right parietal-temporal cortex and the bone flap was removed. The piston was centered 2.5 mm caudal to the bregma and 2 mm lateral to the sagittal suture. Using a stereotaxic impactor (Impact One™; myNeuroLab.com), a 3 mm diameter tip was accelerated to a 1 mm depth at a speed of 5 m/s. Sham operated mice received the same procedure as the TBI mice but omitting the cortical impact.

2.3 | Behavioral testing

To test the ability of mice to exhibit sustained muscle tension opposing the gravitational force associated with their body mass, we used the inverted grid test.³³ Latency to fall from the elevated wire grid was measured three times per session prior to and for 8 consecutive weeks following surgery ±CCI with an inter-trial interval of 30 s. The holding impulse (HI) was calculated as the longest latency to fall out of the three trials per session (holding time) multiplied by the body weight prior to and for 8 consecutive weeks following surgery.

We used the open field activity test to measure exploration and locomotor behavior in mice.³⁴ Following habituation in the testing room, the mice were placed into a square white plexiglass open field box arena and left to move freely for 10 min. Their movement was recorded by a computerized video-tracking system software (Noldus XT 7.1) and analyzed for the distance moved, speed of locomotion, and the transitions between the center and the periphery of the arena.

To examine learning and memory, we used the fear conditioning paradigm.³⁵ Training started with a 2-min acclimation period followed by three consecutive trials consisting of 30-s long auditory tones co-terminating with a foot shock. The inter-trial intervals lasted 30 s. Contextual conditioning was tested 24 h later. Mice were placed into the operand chamber and freezing measured (ANY-MAZE, San Diego Instruments) for a period of 8 min. This was followed 24 h later with testing cued conditioning, which consisted of a 3-min acclimation period prior to a 30-s long presentation of an auditory tone.

2.4 | Immunohistochemistry

Brains were fixed in 4% paraformaldehyde (PFA) and later cut into 10- μ m sections. Sections were blocked and then incubated overnight with primary antibodies against glial fibrillary acidic protein (GFAP; Abcam, ab53554, 1:1000), *Iba1* (Abcam, ab178846, 1:2000), MAP2 (Millipore, AB5622, 1:500), SMI31 (Covance, SMI31R-100, 1:300), and Synapsin 1 (Abcam, ab254349, 1:1000). The following day, the sections were incubated with the secondary antibodies (Life Technologies, A11056, A21206, A21245, A11030, A31573, 1:500, respectively) followed by DAPI (4',6-diamidino-2-phenylindole) staining and Mowiol mounting. Sections stained with secondary antibodies only were used as operational negative controls. Three brain sections per animal were imaged using a 10 \times objective on an AxioScan.Z1 slide scanner (Zeiss) or using

RESEARCH IN CONTEXT

- 1. Systematic review:** We searched online databases for studies reporting roles of amyloid precursor protein (APP) in the control of gene expression. While several previous studies implicated APP in gene expression, we found no experiments investigating whether APP responds to traumatic brain injury (TBI) by changing gene expression.
- 2. Interpretation:** Our experiments reveal an intricate relationship between APP and molecular networks orchestrating brain development and repair, which share similarities at a transcriptional and translational level. The results also suggest that APP responds to TBI by regulating gene expression.
- 3. Future directions:** Mechanisms by which APP controls gene expression in brain development and repair need to be elucidated. APP fragments and domains involved in gene expression need to be clearly identified. These findings will open new avenues for designing therapies for TBI and in providing a more comprehensive understanding of the pathogenesis of Alzheimer's disease (AD).

a 63 \times oil-immersion objective on a confocal laser scanning microscope (LSM780, Zeiss). For the analysis of the slide scanner acquired images, the regions of interest (ROIs) were manually delineated to determine their region sizes for measurements. Quantification was done using Image Pro Premier 3Dsoftware (v9.2). Mean signal (lumen), immunoreactive surface area (%), object density (OD) (number of objects/mm²), and integrated optical density (lumen \times μ m²) were determined for all markers, labeled area percentage, and OD relative to the ROI size. Morphological changes between treatments and genotypes were assessed independently also by a board-certified neuropathologist (C.L.-S.).

2.5 | Western blot

10 μ g of proteins per mouse brain were boiled for 5 min at 95°C in sample buffer (BioRad, 4 \times Laemmli Sample Buffer #1610747), separated using TGX precast gels (BioRad) and transferred onto polyvinylidene fluoride (PVDF) membranes using the semidry Turbo transfer (BioRad). Membranes were then blocked and incubated with primary antibodies against APP (ab126732 Abcam), total tau (ab80579 Abcam), tau T231 (ab151559 Abcam), tau AT8 (MN1020 Invitrogen), tau S416 (Cell Signaling D7U2P #15013), and β -actin (Sigma A5316). The next day, the membranes were incubated with horseradish peroxidase (HRP) -conjugated secondary antibodies and then developed with enhanced chemiluminescence (ECL; BioRad, Clarity, 1705060) and visualized using Chemidoc (BioRad). Protein levels were quantified based on the chemiluminescence signal using ImageJ2 software.

2.6 | RNA sequencing

Illumina RNA sequencing was carried out at the Novogene Bioinformatics Technology Co. (Cambridge, UK). Brain tissue (half of the ipsilateral side of the TBI) was weighed and homogenized in QIAzol lysis reagent (Qiagen) using a microtube homogenizer (# D1030, Bead-Bug, Benchmark Scientific) and processed for RNA extraction with the RNeasy Lipid Tissue Mini Kit (# 74804, Qiagen) as per manufacturer instructions. RNA was checked for quality and degradation via Agilent Bioanalyzer before Illumina sequencing. Sequencing libraries were generated using the NEBNext1 Ultra RNA Library Prep Kit for Illumina1 (New England Biolabs, Ipswich, MA, USA). The library preparations were sequenced on an Illumina HiSeq™ 2000 platform (San Diego, CA, USA).

2.7 | Quantitative real-time polymerase chain reaction analysis

The total RNA was extracted from mouse brains using the RNeasy mini kit (Qiagen). Concentration of isolated RNAs kept at 4°C was determined using Nanodrop 2000c (Thermo scientific, version: 1.4.1). A total of 500 mg of RNA were used for the synthesis of cDNA with Reverse Transcription Reagents kit (Roche Applied Biosystems). cDNA was used as template for the quantitative polymerase chain reaction (qPCR) using Real-Time PCR system (BioRad) with Power SYBR Green PCR Master Mix (Roche). The primers used are listed in the accompanying table (Extended Data Table 1). Gene expression was analyzed using the 2^{-CT} method. All results were normalized to the expression of *RPL13* and *RPL27* housekeeping genes. Each sample was examined using three biological and three technical replicates. For validation, the qPCR data were calculated as log₂-fold changes and compared with log₂-fold values obtained from RNAseq (Extended Data Table 1, Extended Data Table 2).³⁶

2.8 | Mass spectrometry

Brain samples (half of the ipsilateral side of the TBI) were analyzed using TMT-labeling and quantitative MS analysis at the Proteomics Core Facility of the European Molecular Biology Laboratory (Heidelberg, Germany). Protein samples underwent isobaric labeling according to the manufacturer's instructions (TMT6plex Isobaric Label Reagent, ThermoFisher) before quantitative LC-MS/MS via UltiMate 3000 RSLC nano LC system (Dionex). The outlet of the analytical column was coupled to an Orbitrap Fusion Lumos Tribrid Mass Spectrometer (ThermoFisher) using the Nanospray Flex ion source in positive ion mode. Full mass scan (MS1) was acquired with mass range 375–1500 *m/z* in profile mode in the orbitrap with resolution of 60,000. Data dependent acquisition (DDA) was performed with the resolution of the Orbitrap set to 15,000. IsobarQuant (DOI: <https://doi.org/10.1038/nprot.2015.101>) and Mascot (v2.2.07) were used to process the acquired data. Only proteins that were quantified with at least two

unique peptides in at least two out of three replicates were considered for the analysis.

2.9 | Gene ontology and pathways

To biological functions of the RNAs and proteins were examined using the gene ontology (GO) enrichment analyses. Functional enrichment of differentially expressed (DE) RNAs was carried out using the WebGestalt Web tool³⁷ and the ShinyGO 0.77. The Benjamini-Hochberg false discovery rate (FDR) correction was used to assess the significance level and a minimum of five genes per ontology were used as a filter prior to pruning the ontologies. The String database was used to predict the protein-protein interaction (PPI) networks.

2.10 | Statistical analyses

Sample size estimates were performed for behavioral studies (expected moderate effect size $f = 0.25$, probability = 0.05 and minimum power = 80%) using G*Power (v.3.1.9.3), which indicated minimum N of 120. We selected 17 to 27 mice per treatment and genotype with a total N of 130. No a priori power analysis was performed for other experiments, four to nine and three mice per treatment and genotype were selected for morphological assessments and transcriptomic/proteomic experiments, respectively. To verify the statistical power of the results, we also performed post-hoc calculations for the HI (using G*Power), RNAseq (using powerCalc function from HESsRNA package) and TMT-MS data (using check.power function from ssizeRNA package). Calculations showed satisfactory power of 90% (0.903) for the HI, 87% (0.871) for RNAseq, and 95% (0.957) for TMT-MS data.

Multi-group differences in behavioral patterns were analyzed using mixed analysis of variance (ANOVA) with post-hoc *t*-test for pairwise comparisons. The obtained *p*-values were adjusted using Benjamini-Hochberg correction for multiple comparisons where appropriate.

2.11 | Differences in morphology, including immunoreactivity and object densities, were analyzed using a series of *t*-tests with Benjamini-Hochberg correction

Heatmaps of DE and principal component analyses (PCAs) were performed first to explore the structure of the “omics” data. Subsequently, DE analyses of the RNA data were carried out using the DESeq R package. The resulting *p*-values were adjusted using the Benjamini and Hochberg approach for controlling the FDR. Genes with an adjusted *p*-value (FDR) < 0.05 were considered DE. qPCR data were analyzed with a two-tailed test and correlations between results obtained with qPCR and RNAseq were performed using a Spearman's rank correlation (Extended Data Table 2). Rank-Rank Hypergeometric Overlap (RRHO) analysis was used to detect and visualize trends in overlapping

gene-expression profiles. Two different approaches were used to identify hub genes. First, a PPI network of interactive relationships between differentially expressed genes (DEGs) was created using CytoScape (StringApp plugin, v.1.7.1) with a strict combined confidence score of ≥ 0.7 used as a threshold. Subsequently, the MCODE plugin (v.2.0.2) was used to perform submodule analysis (with a degree value ≥ 4 as threshold). CytoScape was then used to construct and visualize the PPI network and to identify the submodules. The modules with most nodes and the highest MCODE scores were considered the hub modules. Second, the CytoHubba plugin (v.0.1) for CytoScape was used to spot hub genes from the PPI network, which identified 50 genes with the highest scores in six commonly used algorithms (Maximal Clique Centrality, Maximum Neighborhood Component, Degree, Closeness, Stress, and Edge Percolated Component). Finally, hub genes captured by all these six algorithms were identified using the UpSetR package in R. The overlaps of the lists of DE RNAs were analyzed using Fisher's exact test.

For proteomics data, pairwise differences in protein levels were identified using the limma package in R applying a linear model using weighted least squares for each protein, calculating differences between groups based on the contrast of the fitted linear models and then applying Empirical Bayes smoothing of standard errors, yielding a moderated t-statistic with Benjamini-Hochberg FDR corrected *p*-values. A threshold of adjusted *p*-value < 0.05 was used to identify differential protein levels. All "omics" results were plotted using the volcano plots generated by the ggplot2 package. Protein/RNA ratio was calculated as the ratio of \log_2 signal sum (for proteins) to gene count (for RNAs) for all proteins identified with TMT-MS and their DE and non-DE matching RNAs. The values were expressed as %. The Kruskal-Wallis test was used to determine differences of molecular weights of the bands. All statistical tests were performed as two-tailed and all $p < 0.05$ (or corresponding $-\log_{10} p > 1.301$) were considered statistically significant. Data analysis was performed in the RStudio (v.2022.07.2 with R v.4.2.1), CytoScape (v.3.9.1), and GraphPad Prism 9 (La Jolla, CA, USA).

3 | RESULTS

3.1 | APP deficiency phenocopies TBI transcriptome

We first compared transcriptional profiles of RNAs purified and sequenced from half of the brain regions harvested ipsilaterally to the site of TBI from WT and APP KO mice following no treatment, sham surgery (Sham), or CCI (Figure 1A). To avoid the confounding effect of the inflammatory and other processes taking place in the immediate aftermath of TBI,^{29,38,39} and to allow testing mice with a battery of behavioral paradigms over time following TBI (Figure S1), we examined transcriptomic profiles in mice 10 weeks following different treatments. Apart from previously reported TBI induced reactive gliosis,^{7,8,40,41} defined as increased GFAP and *Iba1* immunoreactivity of the astrocytes and microglia,⁴² respectively, brains showed no sig-

nificant changes in size nor gross differences in morphology between treatments and genotypes (Figure S2, S3, S4, Extended Data Table 3, Extended Data Table 4, Extended Data Table 5, Extended Data Table 6, Extended Data Table 7, Extended Data Table 8, Extended Data Table 9). In agreement with previous work,¹¹ we also found no reactive gliosis in APP-deficient mice. Given small sample size, modest differences in morphology cannot be fully excluded.

The heatmap and the PCA demonstrated significant differences between treatments and genotypes with differences validated using quantitative real-time PCR (Figure 1B,C, Table S1B, Figure S5A,B). A total of 2862/18,012 (15.9%) brain RNAs were DE in WT-TBI compared with WT mice (Figure 1D, Table S1D). In stark contrast, only 74/17,475 (0.4%) and 256/16,939 (1.5%) brain RNAs were DE in KO-TBI compared with KO or WT-TBI mice, respectively. Unexpectedly, 1745/18,548 (9.4%) brain RNAs were DE in KO compared with WT mice. While this finding corroborates previous reports that APP plays a role in transcription,²⁶ the lack of DE brain RNAs in KO-TBI compared with KO as well as WT-TBI mice suggests that the baseline transcriptome in KO mice largely phenocopies the one observed in WT-TBI mice.

To learn about functions of DE brain RNAs following TBI and APP deficiency, we used GO enrichment analysis. Brain RNAs DE in WT-TBI and KO compared with WT mice were both predicted to upregulate oxidoreductase activity and amide metabolism and to downregulate neurogenesis, neuron differentiation, and projection development (Figure 1E, Table S1E). Mitochondrial organization and processes were predicted to be upregulated in both, but preferentially in KO compared with WT mice. Conversely, brain RNAs DE predominantly in KO versus WT mice were predicted to positively impact dynein intermediate chain and ribosomal components and to diminish GTPase binding activity (Figure 1E, Table S1E). Intriguingly, there were twice as many DE brain RNAs encoding ribosomal proteins in KO compared with WT-TBI mice (Figure S6, Extended Data Table 10). The predicted functional changes corresponding to DE brain RNAs reveal that 10 weeks following TBI, WT mice exhibit enhanced brain metabolism and reduced neuronal regenerative capacity. KO mice share these functional changes with WT-TBI mice in addition to exhibiting distinctive features such as enriched ribosomal activities.

3.2 | Key hub genes in APP deficiency and following TBI encode proteins centered around ribosomes

To further characterize the analogies between DE brain RNAs observed in WT-TBI and KO compared with WT mice, we used the RRHO analysis (Figure 2A). Since many brain RNAs were found DE in WT-TBI versus WT, while there were almost no DE brain RNAs in KO-TBI versus KO, comparison of DE brain RNAs between WT and KO mice following TBI showed predictably incongruous RNA expression profiles. On the contrary, DE brain RNAs in WT-TBI versus WT compared with KO versus WT mice showed congruous RNA expression profiles and thus a concordant RRHO. This analysis corroborated the

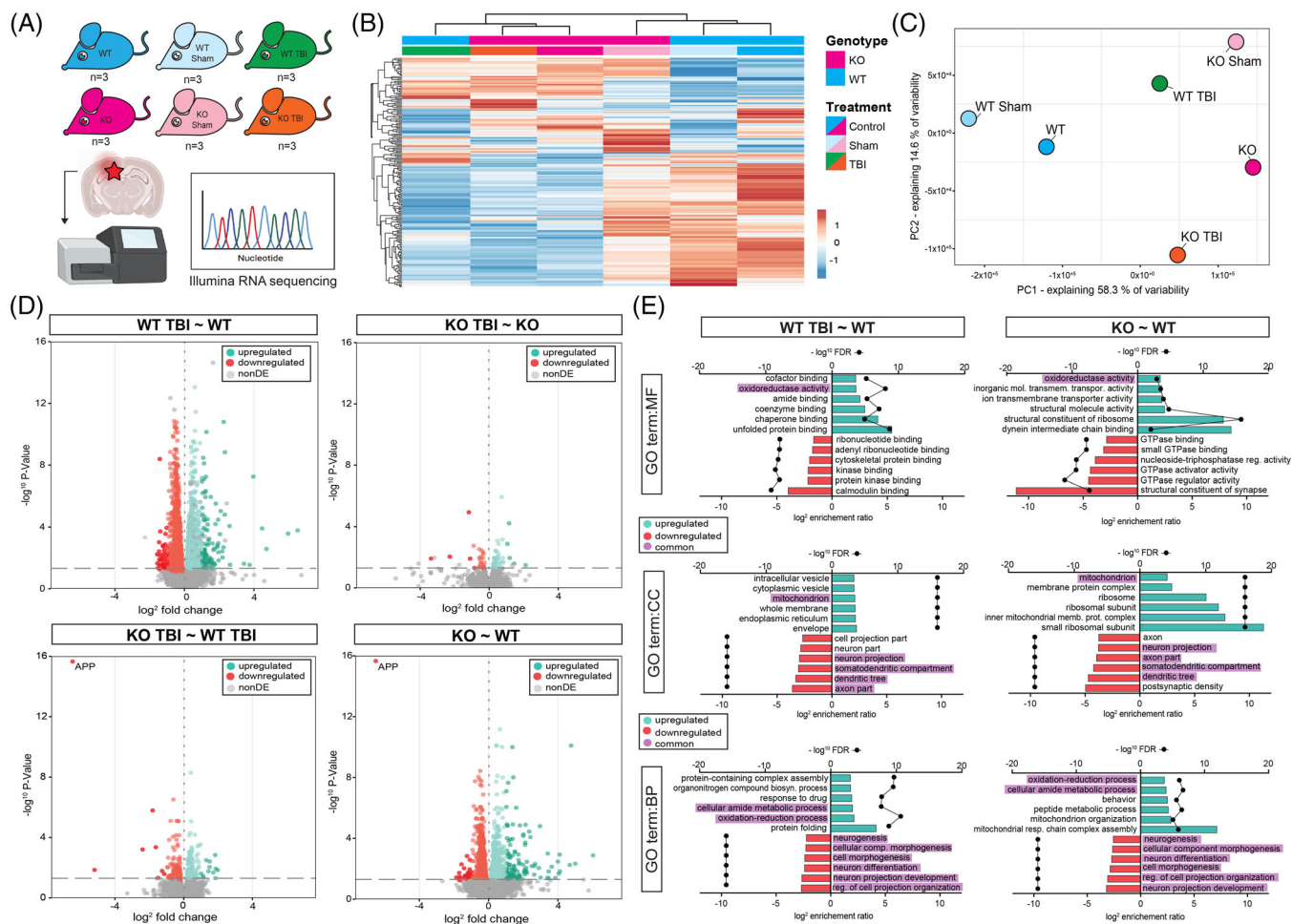


FIGURE 1 Mouse brain transcriptome changes caused by APP deficiency mimicking changes occurring after TBI in WT mouse brains. (A) Schematic of the experimental design of the transcriptomic study. (B) Heatmap depicting transcriptomic profiles between treatments and genotypes. (C) PCA of the transcriptomic profiles of WT, KO, WT-Sham, KO-Sham, WT-TBI, and KO-TBI mice. (D) Volcano plots showing DE brain RNAs in WT-TBI versus WT, KO-TBI versus KO, WT-TBI versus KO-TBI, and WT versus KO mice based on DESeq DGE analysis. Dotted vertical lines indicate the \log_2 fold change of ± 1 . (E) Functional network of significantly enriched GO terms within MF, CC, and BP compared in WT-TBI and KO compared with WT mice. GO analysis included all DE genes. APP, amyloid precursor protein; BP, biological processes; CC, cellular components; DE, differentially expressed; DGE, differential gene expression; FDR, false discovery rate; GO, gene ontology; KO, knock-out; MF, molecular functions; PCA, principal component analysis; TBI, traumatic brain injury; WT, wild-type.

observed transcriptomic analogies by showing similarities in the magnitude and direction of DE brain RNAs between WT-TBI and KO mice. Further data analysis found that these similarities stem from the fact that 1046/1745 (59.9%) DE brain RNAs in KO versus WT mice correspond to DE brain RNAs found in WT-TBI versus WT mice (Figure 2B, Table S2B).

To learn about functions of DE brain RNAs common to WT-TBI and KO mice, we built a PPI network. The PPI network revealed that DE brain RNAs common to WT-TBI and KO mice encode proteins that center functionally around three major clusters. Two clusters consisted of upregulated RNAs predicted to be involved in ribosomal and mitochondrial activity. The third cluster was composed of downregulated RNAs predicted to play roles in neuronal trafficking and transmission (Figure 2C, Table S2C). In agreement with prior work on voltage-gated potassium channels in KO mice,¹¹ brain *Kcnq2* RNA was found to be downregulated in both KO and WT-TBI compared

with WT mice, while brain *Kcnq3* and *Kcnq5* RNAs were downregulated only in WT-TBI. We next used the PPI network to search for hub proteins encoded specifically by brain RNAs DE in both WT-TBI and KO compared with WT mice. We identified 50 candidate hub proteins based on the overlapping network centrality predictions obtained using several topological algorithms. After determining the intersections of the UpSet plot, 10 hub proteins were captured by all six algorithms. Most of these were upregulated and coded for 60S and 40S ribosomal proteins, while those encoding 60S ribosomal protein L29, glutamate receptor subunit zeta 1, and plectin were downregulated (Table S2D). GO enrichment analysis showed that most of the hub proteins are predicted to be involved in biological processes involved in ribosomal small subunit biogenesis, positive regulation of translation, translation, peptide biosynthetic process, peptide metabolic process, and regulation of translation (Figure 2D). In conclusion, these analyses found significant similarities between transcriptional

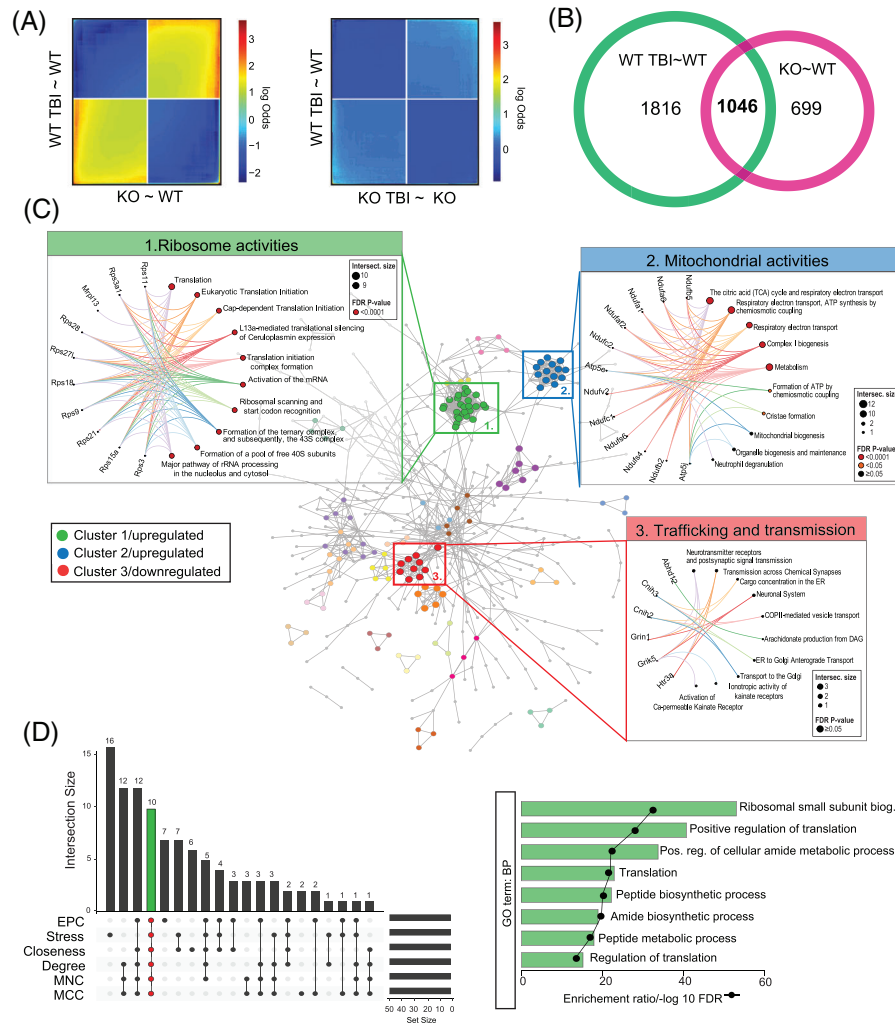


FIGURE 2 Hub genes involved in brain repair after TBI encode ribosomal components and overlap with those affected by APP deficiency. (A) Heatmaps showing \log_2 -transformed odds ratios of rank-rank hypergeometric overlap analysis of concordance of DE brain RNAs between WT-TBI versus WT and KO versus WT and between WT-TBI versus WT and KO-TBI versus KO mice. (B) Venn diagram showing the overlap in DE brain RNAs between WT-TBI versus WT and KO versus WT mice. (C) PPI network of 1046 DE brain RNAs in both WT-TBI and KO versus WT mice with color differentiation of MCODE-derived submodules. A hierarchical clustering network summarizes the relationship between enriched pathways. Bigger dots indicate more significant p -values. (D) UpSet plot showing the overlap of sets of 50 hub genes identified by the 6 CytoHubba plugin algorithm in the PPI network (1046 brain RNAs both in WT-TBI and KO mice) with highlighted 10 hub genes present in all algorithms (EPC, Stress, Closeness, Degree, MNC, and MCC). The most significantly enriched GO terms of BP of the 10 hub genes. APP, amyloid precursor protein; BP, biological processes; DE, differentially expressed; EPC, edge percolated component; FDR, false discovery rate; GO, gene ontology; KO, knock-out; MCC, maximal clique centrality; MNC, maximum neighborhood component; PPI, protein-protein interaction; TBI, traumatic brain injury; WT, wild-type.

profiles of WT-TBI and KO mice, which all revolve primarily around translation.

3.3 | APP deficiency abrogates translation independently from TBI

Considering transcriptomic profiles revealed that translation is the predominant function impacted by the key hub genes identified following TBI and in APP deficiency, we performed TMT-MS using the other half of the brain regions ipsilateral to the site of CCI to investigate

whether and how these transcriptomic profiles affect brain proteome (Figure 3A). The heatmap and PCA found significant quantitative differences among 4316 TMT-MS brain proteins identified in mice following different treatments and genotypes (Figure 3B,C, Table S3B). Only 70 brain proteins (1.6%), however, showed significant quantitative changes in WT-TBI compared with WT mice (Figure 3D, Table S3D). Based on the GO enrichment analysis, proteins with increased brain levels were either members of intermediate filament or myelin sheath protein families, while those exhibiting decreased levels belonged to spectrin-associated cytoskeleton and axonal, including presynaptic, protein families (Figure 3E, Table S3E). This was further confirmed

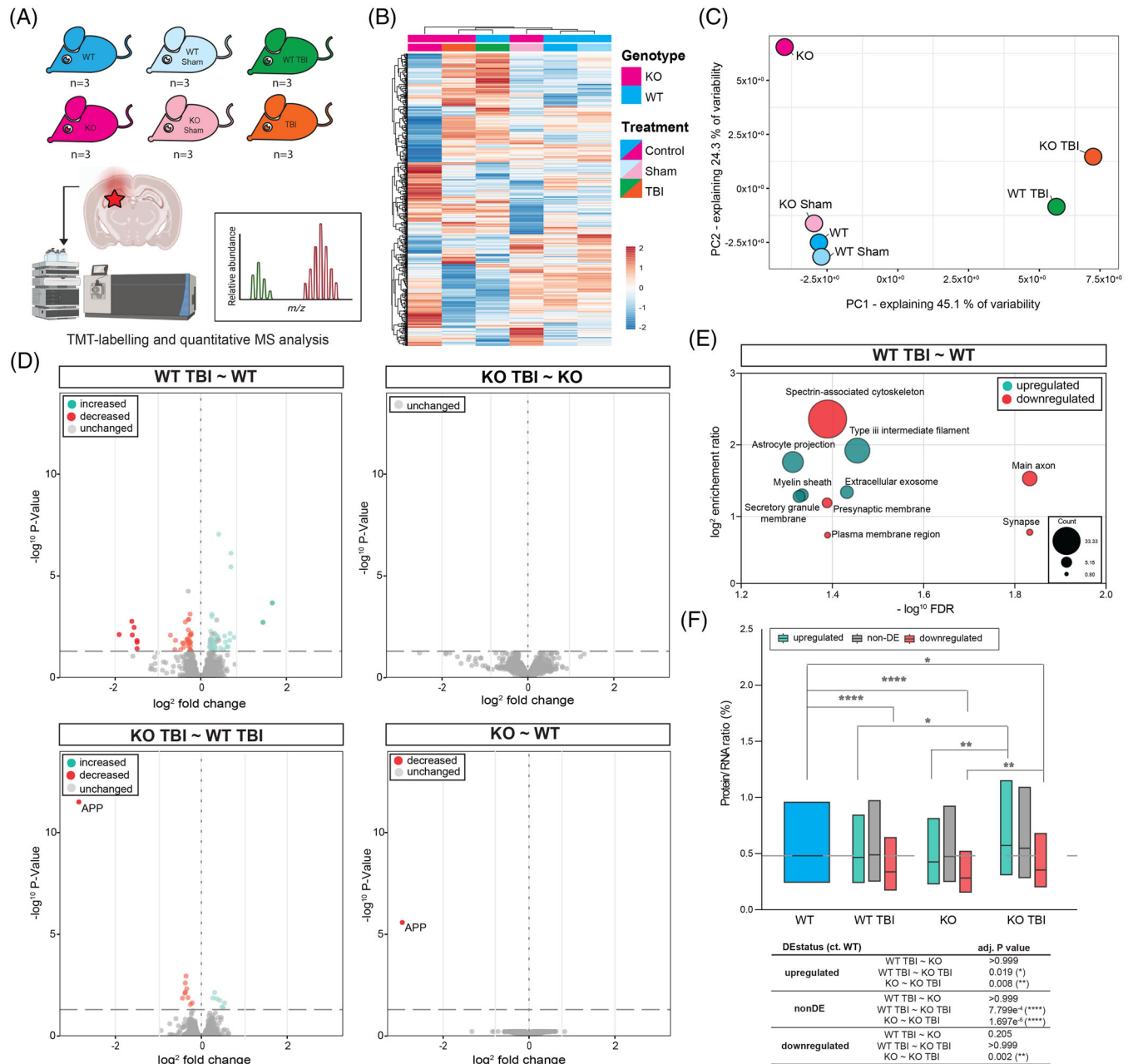


FIGURE 3 APP-deficient mice show no brain proteome changes following TBI. (A) Schematic of the experimental design of the proteomic study. Ipsilateral sides of the brains from mice with different treatments and genotypes were collected to quantify proteins using TMT-MS. (B) Heatmap depicting proteomic profiles from treatments and genotypes. (C) PCA of the proteomic profiles of WT, KO, WT-Sham, KO-Sham, WT-TBI, and KO-TBI mice. (D) Volcano plots showing quantitative protein changes in WT-TBI versus WT, KO-TBI versus KO, WT-TBI versus KO-TBI, and WT versus KO mice. Dotted vertical lines indicate the \log_2 fold change of ± 1 . (E) Functional network of significantly enriched GO terms within CC changed in both TBI exposed WT-TBI compared with WT mice. GO analysis included 32 downregulated and 38 upregulated DE genes. (F) Protein/RNA ratios based on all proteins identified with TMT-MS and their DE and non-DE matching RNAs. Boxplots show protein/RNA ratio (\log_2 signal sum/gene count) of each genotype and treatment compared with the WT mice. Differences were examined using the Wilcoxon test with Benjamini-Hochberg p -value correction (* $p < 0.05$, ** $p < 0.01$, *** $p < 0.001$). APP, amyloid precursor protein; CC, cellular components; DE, differentially expressed; FDR, false discovery rate; GO, gene ontology; KO, knock-out; PCA, principal component analysis; TBI, traumatic brain injury; TMT-MS, tandem mass tag mass spectrometry; WT, wild-type.

studying 28 proteins that following TBI showed changes in parallel with their RNA expression (Figure S7A and Extended Data Table 11). Proteins exhibiting increased brain levels and upregulated RNA were all involved in intermediate filament organization, glial cell development and in vesicle fusion regulation, while proteins with decreased brain levels and downregulated RNA played roles in neuronal projection, development and differentiation (Figure S7B, Extended Data Table 12). In stark contrast, there were no significant protein changes between KO-TBI and KO mice and only 17 proteins (0.4%) showed significant changes in KO-TBI compared with WT-TBI mice. Proteins with increased brain levels included programmed cell death protein 4, sorting nexin 32, contactin 4 and GDNF family receptor $\alpha 2$, while those with decreased brain levels consisted of cytochrome C oxidase subunits, complement C1q, cystatin, and the cannabinoid receptor 1 in addition to the lack of APP (Table S3D). In agreement with more extensive changes in DE brain RNAs encoding ribosomal proteins in KO compared with WT-TBI mice, KO mice showed no brain protein changes compared with WT mice, which indicated that the impact of APP deficiency on translation and brain proteome differs from TBI.

In the attempt to get an insight into differences in the impact of TBI and APP deficiency on brain proteome, we estimated transcriptional-translational coupling by calculating ratios between protein levels and their corresponding RNA expressions (Figure 3F, Table S3F). For downregulated RNAs, we observed a stable pattern of reduced protein/RNA ratios in all WT-TBI, KO, and KO-TBI compared with WT mice. This indicates that reduced RNA profiles following TBI, KO or both lead to reduced protein/RNA ratios suggesting impaired transcriptional-translational coupling. Discrepancies in proteomic changes between WT-TBI (showing modest changes) and KO mice (showing no changes) are consistent with significantly increased DE brain RNAs encoding ribosomal proteins in KO compared with WT-TBI mice and suggest differences in the magnitude by which APP deficiency and TBI impact transcriptional-translational coupling. Conversely, KO-TBI mice exhibited increased protein/RNA ratios in all RNAs compared with KO mice. Predictably, subsets of upregulated and unchanged RNAs in KO-TBI mice also showed increased protein/RNA ratio compared with WT-TBI mice. The combination of diametrically opposite and more extensive changes in protein/RNA ratios accompanied by a lack of any changes in the brain proteome in KO-TBI compared with WT-TBI mice points to mechanistic differences in the transcriptional-translational coupling.

3.4 | APP deficiency mimics inverted grid behavior observed following TBI

To examine whether molecular changes following TBI and APP deficiency translate into any behavioral changes, we tested mice following different treatments and genotypes on a battery of behavioral paradigms over a period of 9 weeks (Figure S1). Compared with WT and WT-Sham mice, WT-TBI mice demonstrated significant impairment in the inverted grid performance throughout the testing period (Figure 4A, Table S4A). KO mice first behaved comparably to WT mice, but then progressively deteriorated on the inverted grid and from

week 13 onward acquired the behavior observed in KO-Sham and all TBI mice. In contrast, KO-TBI mice behaved similarly to WT-TBI mice throughout the testing period. This experiment revealed significant similarities between WT-TBI and KO mice in their inverted grid performance and lack of further deterioration in inverted grid in KO mice following TBI, which contrasted with the APP deficiency-specific behavioral deficits observed in the open field test in which all KO mice showed similar moving duration, but reduced activity in the center and in zone transitions (Figure 4B, Table S4B). In fear conditioning, all mice learned to associate unconditional with conditional stimulus, and performed equally well on contextual and cued conditioning (Figure 4C, Table S4C). Collectively, these experiments show that both KO and KO-TBI mice mimic behavior of WT-TBI mice on the inverted grid, besides exhibiting previously documented genotype specific and TBI-independent "post-traumatic stress disorder" like deficits on other behavioral paradigms.^{7,8,43}

4 | DISCUSSION

During the first weeks following injury, the nervous tissue transiently resets its transcriptional programs to a developmental like "regenerative" state to promote repair prior to reverting to the adult state.⁴⁴ Attenuated neurogenesis, neuron differentiation and projection development 10 weeks following injury correspond to late stages of repair, when the brain has, for the most part, exited the "regenerative" state. These late stages also coincide with time-sensitive transcriptional programs^{45,46} revolving around translational regulation⁴⁷ that are accompanied by decreased protein/RNA ratios and concur with limited changes in brain proteome. Proteomic changes reflect glial and axonal activities predicted to be supported by enhanced brain metabolism.⁴⁸⁻⁵⁰ In this time point of brain repair, mice regain significant capacity for learning and memory but continue displaying sensorimotor deficits.^{51,52}

In stark contrast, APP-deficient mice subject to injury show no brain transcriptional nor proteomic changes. While modest changes could be missed due to small sample size, at least two explanations of this unexpected finding can be entertained. First, similarities in transcriptional profiles between APP-deficient and WT mice following trauma suggest that APP deficiency switches on all the programs relevant to injury independently from injury. Accordingly, the brain becomes molecularly unresponsive to injury since injury-related changes have already been maximally activated. Second, following trauma, APP-deficient mice exhibit a paradoxical increase in protein/RNA ratios, which is diametrically opposite of what is found in both APP-deficient and brain-injured WT mice. This observation supports a view that APP-deficient mice respond to trauma by employing different mechanisms of transcriptional and translational regulation compared with WT mice.

Transcriptional programs in APP deficiency are surprisingly akin to the ones observed in WT mice following injury, with attenuated neurogenesis, neuron differentiation and projection development. This observation suggests that APP deficiency precludes complete brain development and therefore maintains the brain perpetually in an

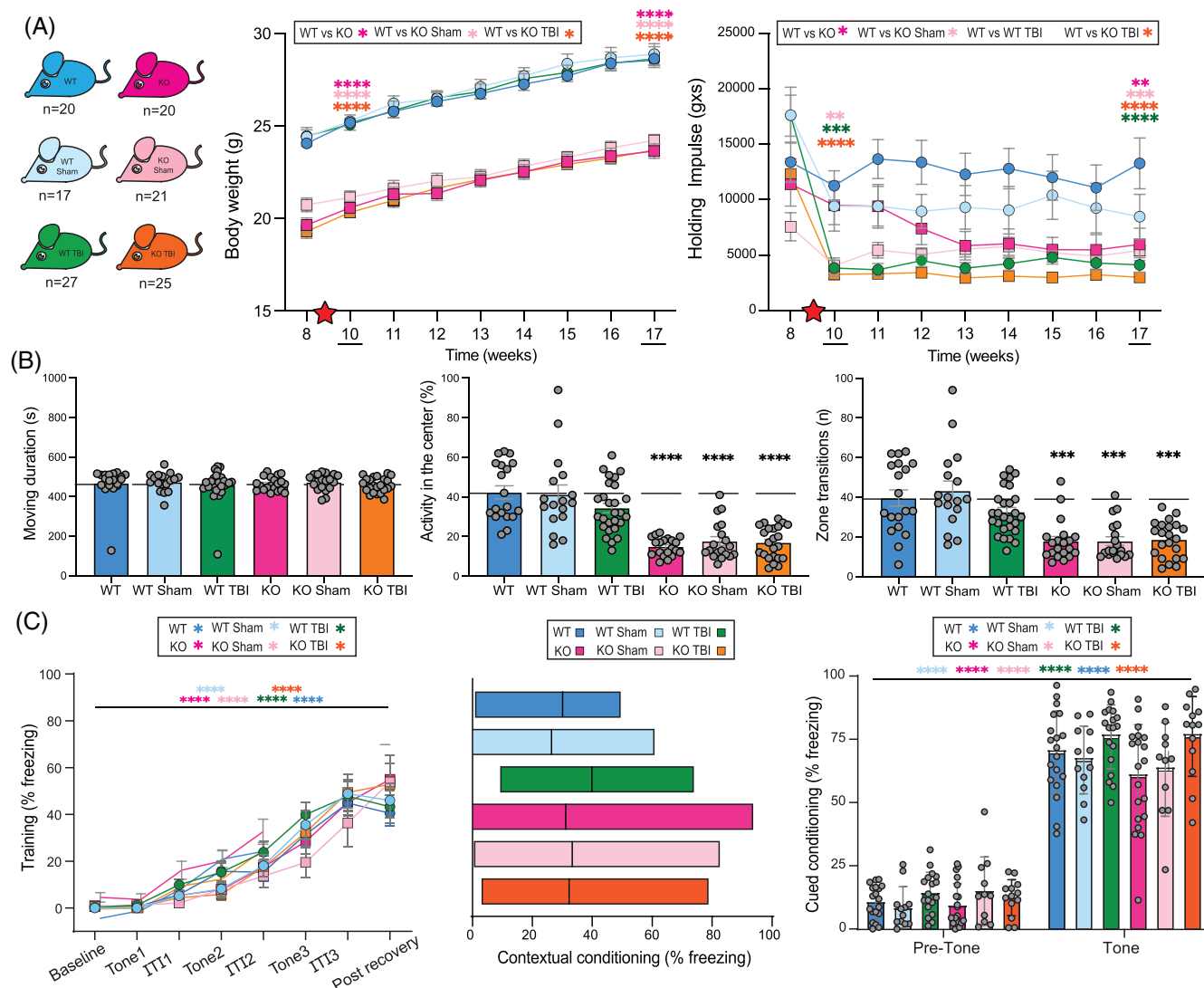


FIGURE 4 APP deficiency mimics inverted grid behavior following TBI. (A) Number of mice used for inverted grid experiments. The average weights and the inverted grid holding impulse scores over the 9 weeks of testing in WT, KO, WT-Sham, KO-Sham, WT-TBI, and KO-TBI mice. Star on the x axis at week 9 marks the time of interventions (surgery, controlled cortical impact). (B) Open field-testing showing mouse performance in moving duration, activity in the center, and in zone transitions (WT $n = 19$, WT-Sham $n = 17$, WT-TBI $n = 27$, KO $n = 20$, KO-Sham $n = 19$, KO-TBI = 23). (C) Fear conditioning showing mouse performance during training and testing contextual (floating bars, min to max, line at mean) and cued conditioning (WT $n = 19$, WT-Sham $n = 13$, WT-TBI $n = 18$, KO $n = 20$, KO-Sham $n = 11$, KO-TBI = 13). Asterisks indicate differences between groups based on mixed ANOVA with post hoc Tukey test and pairwise differences based on t -test with Benjamini–Hochberg p -value correction for multiple comparison ($*p < 0.05$, $**p < 0.01$, $***p < 0.001$, $****p < 0.0001$). ANOVA, analysis of variance; APP, amyloid precursor protein; ITI, intertrial interval; KO, knock-out; TBI, traumatic brain injury; WT, wild-type.

immature state. This is consistent with the role of APP in brain development and in brain disorders.^{12,53} Similar to WT mice following injury, the altered transcriptional repertoire of APP-deficient brains centers around mitochondrial homeostasis and cellular trafficking and transmission, all activities previously linked to APP,^{54–56} and in particular around translational regulation, which shows more extensive changes in APP-deficient compared with brain-injured WT mice. Given the translational effects, it is not surprising that APP deficiency, irrespective of injury, precludes changes in the brain proteome. APP-deficient mice also retain significant capacity for learning and memory but exhibit genotype-specific “post-traumatic stress disorder” like behav-

ior and demonstrate sensorimotor deficits like WT mice following trauma.⁵⁷

The number of genes shown to be regulated by APP is continuously increasing.^{26,58–62} All the proposed mechanisms by which APP regulates gene expression involve formation of complexes between AICD and different scaffolding and adaptor proteins.^{23–25,63–66} Some experiments also suggest that AICD can bind directly to promoter regions of the genes it regulates.⁵⁹ Reported increases in proteolytic APP fragments following brain injury predict increased generation of AICD,^{29,67–70} which is consistent with the role of APP in regulating gene expression in the aftermath of trauma. How APP deficiency

reproduces transcriptional programs observed in WT mice following injury, however, remains unknown. Although significant work is required to answer this question, the observation that inactivation of all APP family members in adulthood results in significantly more restrictive transcriptional changes²⁶ suggests that developmental APP inactivation is required to phenocopy transcriptional changes of brain-injured WT mice.

While several studies report that brain injury reduces translational activities following trauma,^{45,47,71,72} there is little knowledge about the role of APP in translation. While upregulation of brain RNAs encoding ribosomal proteins following brain injury, and in particular in APP deficiency, suggests that both conditions control gene expression by impacting stoichiometry between ribosomal components and perturbing the structure, stability, and function of the ribosome,^{73–75} several mechanisms have been proposed by which APP controls gene expression directly. These include a role of APP in regulating translation via the second internal ribosome entry site and participation of immediate AICD precursor fragments of APP in ribosome-associated quality control.^{71,72,76,77} Although the role of translational regulation in controlling synaptic plasticity and animal behavior is well documented,^{57,78} whether these mechanisms underlie sensorimotor deficits observed following brain trauma and APP deficiency remains to be investigated.

The intricate relationships identified between brain injury and APP deficiency present significant translational potential. Delaying transcriptional and proteomic changes in response to deleterious effects of molecules released following injury by transient APP reductions might be of clinical benefit and should be further investigated. The observation that APP-deficient brains are locked in a perpetual state of developmental immaturity corroborates previously proposed roles of APP in brain development,^{12,53,79} cell survival and growth,^{80,81} and synaptic plasticity^{18,82,83} and opens new avenues to understanding the functional roles of different APP fragments.¹⁹ The neuroprotective roles of the secreted APP fragments in brain repair following trauma and other injuries have already been explored,^{84–86} while similar roles for AICD remain to be investigated. Changes in APP have been reported in Alzheimer's disease,^{28,56,87,88} amyloid angiopathies,^{89,90} Down's syndrome^{91,92} and developmental disorders,^{53,93} in addition to brain trauma.^{28–30} A better functional understanding of different APP fragments is therefore bound to elucidate further mechanisms underlying the pathogenesis of several neurological disorders and unveil novel approaches to their therapeutics. For example, mechanisms governing translation have long been reported to be impaired in Alzheimer's disease brains.^{94–96} The emerging role of APP in control of gene expression raises the question of whether changes in translation result from aberrant levels and distribution of APP fragments, which would then be relevant to the pathogenesis of Alzheimer's disease or represent mere repercussions of its hallmark pathologies.

ACKNOWLEDGMENTS

We are grateful to the past and current members of the Stokin Lab for their valuable feedback. We thank Dr Robert Zorec, University of Ljubljana, Dr Ken Moya, College de France, Dr

Liam Keegan, Central European Institute of Technology and Dr Emanuele Buratti, International Centre for Genetic Engineering and Biotechnology, for their comments regarding the experiments presented in this manuscript. The European Regional Development Funds No. CZ.02.1.01/0.0/0.0/16_019/0000868 ENOCH grant (G.B.S.), The European Union's Horizon 2020 research and innovation programme under grant agreement No. 857560 and CZ.02.1.01/0.0/0.0/17_043/0009632 CETOCOEN EXCELLENCE Teaming grant (G.B.S.), No. CZ.02.1.01/0.0/0.0/15_003/0000492 MAGNET (G.B.S.), the VA Merit Award (5I01BX003671) (B.P.H.) and VA Research Career Scientist Award (1IK6BX006318) (B.P.H.), The Czech Science Foundation (GAČR) Grant Number: 21-27329X (V.L.), European Union: Next Generation EU – Project National Institute for Neurological Research (LX22NPO5107 (MEYS)) (G.B.S.).

CONFLICT OF INTEREST STATEMENT

The authors report no competing interests. Author disclosures are available in the [Supporting Information](#).

ETHICS STATEMENT

WT (C57BL/6) and APP KO (B6.129S7-App^{tm1Dbo}/J) backcrossed to C57BL/6 mice were purchased from Jackson Laboratories (Bar Harbor, ME, USA) and handled in compliance with the Guide for the Care and Use of the Laboratory Animals (National Academy of Science, Washington DC, USA). All animal use protocols were approved by the Veterans Administration San Diego Healthcare System Institutional Animal Care and Use Committee (San Diego, CA, USA), approval number 14-044.

REFERENCES

- Dyrks T, Weidemann A, Multhaup G, et al. Identification, transmembrane orientation and biogenesis of the amyloid A4 precursor of Alzheimer's disease. *EMBO J*. 1988;7:949-957. doi:10.1002/j.1460-2075.1988.tb02900.x
- Wasco W, Bupp K, Magendanz M, Gusella JF, Tanzi RE, Solomon F. Identification of a mouse brain cDNA that encodes a protein related to the Alzheimer disease-associated amyloid beta protein precursor. *Proc Natl Acad Sci U S A*. 1992;89:10758-10762. doi:10.1073/pnas.89.22.10758
- Wasco W, Gurubhagavatula S, Paradis MD, et al. Isolation and characterization of APLP2 encoding a homologue of the Alzheimer's associated amyloid beta protein precursor. *Nat Genet*. 1993;5:95-100. doi:10.1038/ng0993-95
- Rosen DR, Martin-Morris L, Luo LQ, White K. A *Drosophila* gene encoding a protein resembling the human beta-amyloid protein precursor. *Proc Natl Acad Sci U S A*. 1989;86:2478-2482. doi:10.1073/pnas.86.7.2478
- Daigle I, Li C. apl-1, a *Caenorhabditis elegans* gene encoding a protein related to the human beta-amyloid protein precursor. *Proc Natl Acad Sci U S A*. 1993;90:12045-12049. doi:10.1073/pnas.90.24.12045
- Musa A, Lehrach H, Russo VA. Distinct expression patterns of two zebrafish homologues of the human APP gene during embryonic development. *Dev Genes Evol*. 2001;211:563-567. doi:10.1007/s00427-001-0189-9
- Zheng H, Jiang M, Trumbauer ME, et al. beta-Amyloid precursor protein-deficient mice show reactive gliosis and decreased locomotor activity. *Cell*. 1995;81:525-531. doi:10.1016/0092-8674(95)90073-x

8. Muller U, Cristina N, Li ZW, et al. Behavioral and anatomical deficits in mice homozygous for a modified beta-amyloid precursor protein gene. *Cell*. 1994;79:755-765. doi:10.1016/0092-8674(94)90066-3
9. Heber S, Herms J, Gajic V, et al. Mice with combined gene knockouts reveal essential and partially redundant functions of amyloid precursor protein family members. *J Neurosci*. 2000;20:7951-7963.
10. von Koch C, Zheng H, Chen H, et al. Generation of APLP2 KO mice and early postnatal lethality in APLP2/APP double KO mice. *Neurobiol Aging*. 1997;18:661-669. doi:10.1016/s0197-4580(97)00151-6
11. Lee SH, Kang J, Ho A, Watanabe H, Bolshakov VY, Shen J. APP family regulates neuronal excitability and synaptic plasticity but not neuronal survival. *Neuron*. 2020;108:676-690. e678. doi:10.1016/j.neuron.2020.08.011
12. Steubler V, Erdinger S, Back MK, et al. Loss of all three APP family members during development impairs synaptic function and plasticity, disrupts learning, and causes an autism-like phenotype. *EMBO J*. 2021;40:e107471. doi:10.15252/embj.2020107471
13. Schubert W, Prior R, Weidemann A, et al. Localization of Alzheimer beta A4 amyloid precursor protein at central and peripheral synaptic sites. *Brain Res*. 1991;563:184-194. doi:10.1016/0006-8993(91)91532-6
14. Furukawa K, Barger SW, Blalock EM, Mattson MP. Activation of K⁺ channels and suppression of neuronal activity by secreted beta-amyloid-precursor protein. *Nature*. 1996;379:74-78. doi:10.1038/379074a0
15. Chapman PF, White GL, Jones MW, et al. Impaired synaptic plasticity and learning in aged amyloid precursor protein transgenic mice. *Nat Neurosci*. 1999;2:271-276. doi:10.1038/6374
16. Marik SA, Olsen O, Tessier-Lavigne M, Gilbert CD. Physiological role for amyloid precursor protein in adult experience-dependent plasticity. *Proc Natl Acad Sci U S A*. 2016;113:7912-7917. doi:10.1073/pnas.1604299113
17. Mehr A, Hick M, Ludewig S, et al. Lack of APP and APLP2 in GABAergic forebrain neurons impairs synaptic plasticity and cognition. *Cereb Cortex*. 2020;30:4044-4063. doi:10.1093/cercor/bhaa025
18. Roch JM, Masliah E, Roch-Leveq AC, et al. Increase of synaptic density and memory retention by a peptide representing the trophic domain of the amyloid beta/A4 protein precursor. *Proc Natl Acad Sci U S A*. 1994;91:7450-7454. doi:10.1073/pnas.91.16.7450
19. Corrigan F, Pham CL, Vink R, et al. The neuroprotective domains of the amyloid precursor protein, in traumatic brain injury, are located in the two growth factor domains. *Brain Res*. 2011;1378:137-143. doi:10.1016/j.brainres.2010.12.077
20. Plummer SL, Corrigan F, Thornton E, et al. The amyloid precursor protein derivative, APP96-110, is efficacious following intravenous administration after traumatic brain injury. *PLoS One*. 2018;13:e0190449. doi:10.1371/journal.pone.0190449
21. Plummer S, Van den Heuvel C, Thornton E, Corrigan F, Cappai R. The neuroprotective properties of the amyloid precursor protein following traumatic brain injury. *Aging Dis*. 2016;7:163-179. doi:10.14336/AD.2015.0907
22. Guénette SY, Chen J, Jondro PD, Tanzi RE. Association of a novel human FE65-like protein with the cytoplasmic domain of the beta-amyloid precursor protein. *Proc Natl Acad Sci U S A*. 1996;93:10832-10837. doi:10.1073/pnas.93.20.10832
23. Cao X, Südhof TC. A transcriptionally [correction of transcriptively] active complex of APP with Fe65 and histone acetyltransferase Tip60. *Science*. 2001;293:115-120. doi:10.1126/science.1058783
24. Kimberly WT, Zheng JB, Guénette SY, Selkoe DJ. The intracellular domain of the beta-amyloid precursor protein is stabilized by Fe65 and translocates to the nucleus in a notch-like manner. *J Biol Chem*. 2001;276:40288-40292. doi:10.1074/jbc.C100447200
25. Baek SH, Ohgi KA, Rose DW, Koo EH, Glass CK, Rosenfeld MG. Exchange of N-CoR corepressor and Tip60 coactivator complexes links gene expression by NF-kappaB and beta-amyloid precursor protein. *Cell*. 2002;110:55-67. doi:10.1016/s0092-8674(02)00809-7
26. Cha HJ, Shen J, Kang J. Regulation of gene expression by the APP family in the adult cerebral cortex. *Sci Rep*. 2022;12:66. doi:10.1038/s41598-021-04027-8
27. Nakagawa Y, Nakamura M, McIntosh TK, et al. Traumatic brain injury in young, amyloid-beta peptide overexpressing transgenic mice induces marked ipsilateral hippocampal atrophy and diminished Aβ deposition during aging. *J Comp Neurol*. 1999;411:390-398.
28. Gentleman SM, Nash MJ, Sweeting CJ, Graham DI, Roberts GW. Beta-amyloid precursor protein (beta APP) as a marker for axonal injury after head injury. *Neurosci Lett*. 1993;160:139-144. doi:10.1016/0304-3940(93)90398-5
29. Pozo Devoto VM, Lacovich V, Feole M, et al. Unraveling axonal mechanisms of traumatic brain injury. *Acta Neuropathol Commun*. 2022;10:140. doi:10.1186/s40478-022-01414-8
30. Chen X, Siman R, Iwata A, Meaney DF, Trojanowski JQ, Smith DH. Long-term accumulation of amyloid-beta, beta-secretase, presenilin-1, and caspase-3 in damaged axons following brain trauma. *Am J Pathol*. 2004;165:357-371. doi:10.1016/s0002-9440(10)63303-2
31. Richter V, Mueche R, Mayer B. How much confidence do we need in animal experiments? Statistical assumptions in sample size estimation. *J Appl Anim Welf Sci*. 2018;21:325-333. doi:10.1080/10888705.2018.1423972
32. Niesman IR, Schilling JM, Shapiro LA, et al. Traumatic brain injury enhances neuroinflammation and lesion volume in caveolin deficient mice. *J Neuroinflammation*. 2014;11:39. doi:10.1186/1742-2094-11-39
33. Carlson CG, Rutter J, Bledsoe C, et al. A simple protocol for assessing inter-trial and inter-examiner reliability for two noninvasive measures of limb muscle strength. *J Neurosci Methods*. 2010;186:226-230. doi:10.1016/j.jneumeth.2009.11.006
34. Walsh RN, Cummins RA. The open-field test: a critical review. *Psychol Bull*. 1976;83:482-504.
35. Limbäck-Stokin K, Korzus E, Nagaoka-Yasuda R, Mayford M. Nuclear calcium/calmodulin regulates memory consolidation. *J Neurosci*. 2004;24:10858-10867. doi:10.1523/JNEUROSCI.1022-04.2004
36. Wang H, Zhou P, Zhu W, Wang F. De novo comparative transcriptome analysis of genes differentially expressed in the scion of homografted and heterografted tomato seedlings. *Sci Rep*. 2019;9:20240. doi:10.1038/s41598-019-56563-z
37. Wang J, Vasaikar S, Shi Z, Greer M, Zhang B. WebGestalt 2017: a more comprehensive, powerful, flexible and interactive gene set enrichment analysis toolkit. *Nucleic Acids Res*. 2017;45:W130-W137. doi:10.1093/nar/gkx356
38. Abdul-Muneer PM, Long M, Conte AA, Santhakumar V, Pfister BJ. High Ca²⁺ influx during traumatic brain injury leads to caspase-1-dependent neuroinflammation and cell death. *Mol Neurobiol*. 2017;54:3964-3975. doi:10.1007/s12035-016-9949-4
39. Jassam YN, Izzy S, Whalen M, McGavern DB, El Khoury J. Neuroimmunology of traumatic brain injury: time for a paradigm shift. *Neuron*. 2017;95:1246-1265. doi:10.1016/j.neuron.2017.07.010
40. Smith DH, Chen X, Pierce JES, et al. Progressive atrophy and neuron death for one year following brain trauma in the rat. *J Neurotrauma*. 1997;14:715-727. doi:10.1089/neu.1997.14.715
41. Dawson G, Seabrook G, Zheng H, et al. Age-related cognitive deficits, impaired long-term potentiation and reduction in synaptic marker density in mice lacking the beta-amyloid precursor protein. *Neuroscience*. 1999;90:1-13. doi:10.1016/s0306-4522(98)00410-2
42. Escartin C, Galea E, Lakatos A, et al. Reactive astrocyte nomenclature, definitions, and future directions. *Nat Neurosci*. 2021;24:312-325. doi:10.1038/s41593-020-00783-4
43. Senechal Y, Kelly PH, Dev KK. Amyloid precursor protein knockout mice show age-dependent deficits in passive avoidance learning. *Behav Brain Res*. 2008;186:126-132. doi:10.1016/j.bbr.2007.08.003

44. Poplawski GHD, Kawaguchi R, Van Niekerk E, et al. Injured adult neurons regress to an embryonic transcriptional growth state. *Nature*. 2020;581:77-82. doi:10.1038/s41586-020-2200-5
45. Zhang L, Yang Q, Yuan R, et al. Single-nucleus transcriptomic mapping of blast-induced traumatic brain injury in mice hippocampus. *Sci Data*. 2023;10:638. doi:10.1038/s41597-023-02552-x
46. Bjorklund GR, Wong J, Brafman D, Bowser R, Stabenfeldt SE. Traumatic brain injury induces TDP-43 mislocalization and neurodegenerative effects in tissue distal to the primary injury site in a non-transgenic mouse. *Acta Neuropathol Commun*. 2023;11:137. doi:10.1186/s40478-023-01625-7
47. PerezGrovas-Saltijeral A, Rajkumar AP, Knight HM. Differential expression of m(5)C RNA methyltransferase genes NSUN6 and NSUN7 in Alzheimer's disease and traumatic brain injury. *Mol Neurobiol*. 2023;60:2223-2235. doi:10.1007/s12035-022-03195-6
48. Di Pietro V, Lazzarino G, Amorini AM, et al. Fusion or fission: the destiny of mitochondria in traumatic brain injury of different severities. *Sci Rep*. 2017;7:9189. doi:10.1038/s41598-017-09587-2
49. Pozo Devoto VM, Onyango IG, Stokin GB. Mitochondrial behavior when things go wrong in the axon. *Front Cell Neurosci*. 2022;16:959598. doi:10.3389/fncel.2022.959598
50. van Hameren G, Muradov J, Minarik A, et al. Mitochondrial dysfunction underlies impaired neurovascular coupling following traumatic brain injury. *Neurobiol Dis*. 2023;186:106269. doi:10.1016/j.nbd.2023.106269
51. Bhowmick S, D'Mello V, Ponery N, Abdul-Muneer P. Neurodegeneration and sensorimotor deficits in the mouse model of traumatic brain injury. *Brain Sci*. 2018;8:11. doi:10.3390/brainsci8010011
52. Egawa J, Schilling JM, Cui W, et al. Neuron-specific caveolin-1 overexpression improves motor function and preserves memory in mice subjected to brain trauma. *FASEB J*. 2017;31:3403-3411. doi:10.1096/fj.201601288RRR
53. Bamford RA, Zuko A, Eve M, et al. CNTN4 modulates neural elongation through interplay with APP. *Open Biol*. 2024;14:240018. doi:10.1098/rsob.240018
54. Lopez Sanchez MIG, Waugh HS, Tsatsanis A, et al. Amyloid precursor protein drives down-regulation of mitochondrial oxidative phosphorylation independent of amyloid beta. *Sci Rep*. 2017;7:9835. doi:10.1038/s41598-017-10233-0
55. Bretou M, Sannerud R, Escamilla-Ayala A, et al. Accumulation of APP C-terminal fragments causes endolysosomal dysfunction through the dysregulation of late endosome to lysosome-ER contact sites. *Dev Cell*. 2024;59(12):1571-1592. e9. doi:10.1016/j.devcel.2024.03.030
56. Feole M, Pozo Devoto VM, Dragišić N, et al. Swedish Alzheimer's disease variant perturbs activity of retrograde molecular motors and causes widespread derangement of axonal transport pathways. *J Biol Chem*. 2024;300:107137. doi:10.1016/j.jbc.2024.107137
57. Carron SF, Yan EB, Alwis DS, Rajan R. Differential susceptibility of cortical and subcortical inhibitory neurons and astrocytes in the long term following diffuse traumatic brain injury. *J Comp Neurol*. 2016;524:3530-3560. doi:10.1002/cne.24014
58. Opsomer R, Contino S, Perrin F, et al. Amyloid precursor protein (APP) controls the expression of the transcriptional activator neuronal PAS domain protein 4 (NPAS4) and synaptic GABA release. *eNeuro*. 2020;7(3):ENEURO.0322-19.2020. doi:10.1523/ENEURO.0322-19.2020
59. Ceglia I, Reitz C, Gresack J, et al. APP intracellular domain-WAVE1 pathway reduces amyloid-beta production. *Nat Med*. 2015;21:1054-1059. doi:10.1038/nm.3924
60. Grimm MOW, Zinser EG, Grösgen S, et al. Amyloid precursor protein (APP) mediated regulation of ganglioside homeostasis linking Alzheimer's disease pathology with ganglioside metabolism. *PLoS One*. 2012;7:e34095. doi:10.1371/journal.pone.0034095
61. Huysseune S, Kienlen-Campard P, Hébert S, et al. Epigenetic control of aquaporin 1 expression by the amyloid precursor protein. *FASEB J*. 2009;23:4158-4167. doi:10.1096/fj.09-140012
62. Shu R, Wong W, Ma QH, et al. APP intracellular domain acts as a transcriptional regulator of miR-663 suppressing neuronal differentiation. *Cell Death Dis*. 2015;6:e1651. doi:10.1038/cddis.2015.10
63. Cao X, Südhof TC. Dissection of amyloid-beta precursor protein-dependent transcriptional transactivation. *J Biol Chem*. 2004;279:24601-24611. doi:10.1074/jbc.M402248200
64. Probst S, Riese F, Kägi L, et al. Lysine acetyltransferase Tip60 acetylates the APP adaptor Fe65 to increase its transcriptional activity. *Biol Chem*. 2021;402:481-499. doi:10.1515/hsz-2020-0279
65. Biederer T, Cao X, Südhof TC, Liu X. Regulation of APP-dependent transcription complexes by Mint/X11s: differential functions of Mint isoforms. *J Neurosci*. 2002;22:7340-7351. doi:10.1523/JNEUROSCI.22-17-07340.2002
66. Araki Y, Miyagi N, Kato N, et al. Coordinated metabolism of Alcadin and amyloid beta-protein precursor regulates FE65-dependent gene transactivation. *J Biol Chem*. 2004;279:24343-24354. doi:10.1074/jbc.M401925200
67. Capone R, Tiwari A, Hadziselimovic A, et al. The C99 domain of the amyloid precursor protein resides in the disordered membrane phase. *J Biol Chem*. 2021;296:100652. doi:10.1016/j.jbc.2021.100652
68. Agrawal RR, Larrea D, Xu Y, et al. Alzheimer's-associated upregulation of mitochondria-associated ER membranes after traumatic brain injury. *Cell Mol Neurobiol*. 2023;43:2219-2241. doi:10.1007/s10571-022-01299-0
69. Van den Heuvel C, Blumbergs PC, Finnie JW, et al. Upregulation of amyloid precursor protein messenger RNA in response to traumatic brain injury: an ovine head impact model. *Exp Neurol*. 1999;159:441-450. doi:10.1006/exnr.1999.7150
70. Hefter D, Draguhn A. APP as a protective factor in acute neuronal insults. *Front Mol Neurosci*. 2017;10:22. doi:10.3389/fnmol.2017.00022
71. Dash PK, Hylin MJ, Hood KN, et al. Inhibition of eukaryotic initiation factor 2 alpha phosphatase reduces tissue damage and improves learning and memory after experimental traumatic brain injury. *J Neurotrauma*. 2015;32:1608-1620. doi:10.1089/neu.2014.3772
72. Chou A, Krukowski K, Jopson T, et al. Inhibition of the integrated stress response reverses cognitive deficits after traumatic brain injury. *Proc Natl Acad Sci U S A*. 2017;114:E6420-E6426. doi:10.1073/pnas.1707661114
73. Petibon C, Malik Ghulam M, Catala M, Abou Elela S. Regulation of ribosomal protein genes: an ordered anarchy. *Wiley Interdiscip Rev RNA*. 2021;12:e1632. doi:10.1002/wrna.1632
74. Sabi R, Tuller T. Modelling and measuring intracellular competition for finite resources during gene expression. *J R Soc Interface*. 2019;16:20180887. doi:10.1098/rsif.2018.0887
75. Metzl-Raz E, Kafri M, Yaakov G, Soifer I, Gurvich Y, Barkai N. Principles of cellular resource allocation revealed by condition-dependent proteome profiling. *Elife*. 2017;6:e28034. doi:10.7554/elife.28034
76. Li M, Pehar M, Liu Y, et al. The amyloid precursor protein (APP) intracellular domain regulates translation of p44, a short isoform of p53, through an IRES-dependent mechanism. *Neurobiol Aging*. 2015;36:2725-2736. doi:10.1016/j.neurobiolaging.2015.06.021
77. Rimal S, Li Y, Vartak R, et al. Inefficient quality control of ribosome stalling during APP synthesis generates CAT-tailed species that precipitate hallmarks of Alzheimer's disease. *Acta Neuropathol Commun*. 2021;9:169. doi:10.1186/s40478-021-01268-6
78. Klann E, Dever TE. Biochemical mechanisms for translational regulation in synaptic plasticity. *Nat Rev Neurosci*. 2004;5:931-942. doi:10.1038/nrn1557

79. Müller UC, Deller T, Korte M. Not just amyloid: physiological functions of the amyloid precursor protein family. *Nat Rev Neurosci*. 2017;18:281-298. doi:10.1038/nrn.2017.29
80. Saitoh T, Sundsmo M, Roch J, et al. Secreted form of amyloid beta protein precursor is involved in the growth regulation of fibroblasts. *Cell*. 1989;58:615-622. doi:10.1016/0092-8674(89)90096-2
81. Kessissoglou IA, Langui D, Hasan A, et al. The *Drosophila* amyloid precursor protein homologue mediates neuronal survival and neuroglial interactions. *PLoS Biol*. 2020;18:e3000703. doi:10.1371/journal.pbio.3000703
82. Meziane H, Dodart J, Mathis C, et al. Memory-enhancing effects of secreted forms of the beta-amyloid precursor protein in normal and amnesic mice. *Proc Natl Acad Sci U S A*. 1998;95:12683-12688. doi:10.1073/pnas.95.21.12683
83. Araki W, Kitaguchi N, Tokushima Y, et al. Trophic effect of beta-amyloid precursor protein on cerebral cortical neurons in culture. *Biochem Biophys Res Commun*. 1991;181:265-271. doi:10.1016/s0006-291x(05)81412-3
84. Clarke J, Thornell A, Corbett D, Soininen H, Hiltunen M, Jolkkonen J. Overexpression of APP provides neuroprotection in the absence of functional benefit following middle cerebral artery occlusion in rats. *Eur J Neurosci*. 2007;26:1845-1852. doi:10.1111/j.1460-9568.2007.05807.x
85. Corrigan F, Vink R, Blumbergs PC, Masters CL, Cappai R, van den Heuvel C. sAPPalpha rescues deficits in amyloid precursor protein knockout mice following focal traumatic brain injury. *J Neurochem*. 2012;122:208-220. doi:10.1111/j.1471-4159.2012.07761.x
86. Ayton S, Zhang M, Roberts BR, et al. Ceruloplasmin and beta-amyloid precursor protein confer neuroprotection in traumatic brain injury and lower neuronal iron. *Free Radic Biol Med*. 2014;69:331-337. doi:10.1016/j.freeradbiomed.2014.01.041
87. Sennvik K, Fastbom J, Blomberg M, Wahlund L, Winblad B, Benedikz E. Levels of alpha- and beta-secretase cleaved amyloid precursor protein in the cerebrospinal fluid of Alzheimer's disease patients. *Neurosci Lett*. 2000;278:169-172. doi:10.1016/s0304-3940(99)00929-5
88. Wu G, Sankaranarayanan S, Hsieh SH, Simon AJ, Savage MJ. Decrease in brain soluble amyloid precursor protein beta (sAPPbeta) in Alzheimer's disease cortex. *J Neurosci Res*. 2011;89:822-832. doi:10.1002/jnr.22618
89. Shinkai Y, Yoshimura M, Ito Y, et al. Amyloid beta-proteins 1-40 and 1-42(43) in the soluble fraction of extra- and intracranial blood vessels. *Ann Neurol*. 1995;38:421-428. doi:10.1002/ana.410380312
90. Van Broeckhoven C, Haan J, Bakker E, et al. Amyloid beta protein precursor gene and hereditary cerebral hemorrhage with amyloidosis (Dutch). *Science*. 1990;248:1120-1122. doi:10.1126/science.1971458
91. Oyama F, Cairns NJ, Shimada H, Oyama R, Titani K, Ihara Y. Down's syndrome: up-regulation of beta-amyloid protein precursor and tau mRNAs and their defective coordination. *J Neurochem*. 1994;62:1062-1066. doi:10.1046/j.1471-4159.1994.62031062.x
92. Jiang Y, Sato Y, Im E, et al. Lysosomal dysfunction in Down syndrome is APP-Dependent and mediated by APP-betaCTF (C99). *J Neurosci*. 2019;39:5255-5268. doi:10.1523/JNEUROSCI.0578-19.2019
93. Song C, Broadie K. Fragile X mental retardation protein coordinates neuron-to-glia communication for clearance of developmentally transient brain neurons. *Proc Natl Acad Sci U S A*. 2023;120:e2216887120. doi:10.1073/pnas.2216887120
94. Hernández-Ortega K, García-Esparcia P, Gil L, Lucas JJ, Ferrer I. Altered machinery of protein synthesis in Alzheimer's: from the nucleus to the ribosome. *Brain Pathol*. 2016;26:593-605. doi:10.1111/bpa.12335
95. Ding Q, Markesbery WR, Chen Q, Li F, Keller JN. Ribosome dysfunction is an early event in Alzheimer's disease. *J Neurosci*. 2005;25:9171-9175. doi:10.1523/JNEUROSCI.3040-05.2005
96. Sajdel-Sulkowska EM, Marotta CA. Alzheimer's disease brain: alterations in RNA levels and in a ribonuclease-inhibitor complex. *Science*. 1984;225:947-949. doi:10.1126/science.6206567

SUPPORTING INFORMATION

Additional supporting information can be found online in the Supporting Information section at the end of this article.

How to cite this article: Lacovich V, Čarna M, Novotný SJ, et al. Developmental deletion of amyloid precursor protein precludes transcriptional and proteomic responses to brain injury. *Alzheimer's Dement*. 2025;21:e70093. <https://doi.org/10.1002/alz.70093>